JOURNAL OF GEOPHYSICAL RESEARCH, VOL. 86, NO. A6, PAGES 4597-4606, JUNE 1, 1981

ELECTRON PRECIPITATION INDUCED BY VLF NOISE BURSTS AT THE PLASMAPAUSE AND DETECTED AT CONJUGATE GROUND STATIONS

Bruce Dingle and D. L. Carpenter

Radioscience Laboratory, Stanford University, Stanford, California 94305

Abstract. A new type of wave-induced electron precipitation event has been identified. During observations at conjugate stations Siple, Antarctica, and Roberval, Canada (L ~4.2), VLF noise bursts were found to be associated on a one-to-one basis with amplitude perturbations of subionospheric radio propagation. The amplitude perturbations are attributed to patches of enhanced ionization that extended below ~80 km in the nighttime ionosphere and that were produced by precipitating electron bursts. Similar amplitude perturbations seen previously were correlated with whistlers that propagated within the plasmasphere. For the new events the driving waves were structured collections of rising elements that propagated just beyond the plasmapause at roughly 5-min intervals over a several-hour period. These noise bursts were of relatively long duration (~10 s) and strong intensity (inferred to be >30 pT at the equator). Triggering of the noise bursts appears to have been mostly by whistlers but changed in character with time. Some later bursts had narrowband precursors at constant frequencies possibly locked to power line harmonic radiation. The burst initiation characteristics suggest the existence of a variable threshold for rapid temporal growth in the magnetosphere controlled by the trapped electron dynamics. The temporal signatures of the amplitude perturbations show that precipitation was maintained over multiple bounces of the trapped magnetospheric electrons. In some cases these signatures included a new undershoot effect during the recovery phase lasting 2-5 min. This effect may have been related to cutoff of background drizzle precipitation. Precipitation effects were observed on both long (~10 Mm) and short (~½ Mm) subionospheric paths and were monitored simultaneously at the conjugate stations. Similarities in the perturbation signatures on long and short paths suggest that the form of the signatures was governed by ionospheric changes and was not distorted by the subionospheric propagation mechanism. Some differences in the conjugate perturbation signatures are believed to be caused by the difference in loss cone widths for precipitation in the northern and southern hemispheres. Existence of this loss cone gap produced an estimated ~30-pT noise amplitude threshold for significant northern precipitation and possibly caused saturation of southern precipitation.

Introduction

VLF-wave-induced burst precipitation of energetic electrons from the magnetosphere at subauroral latitudes has been detected by several means in recent years. The methods used have included comparisons of VLF wave activity with X rays observed on balloons [e.g. Rosenberg et al., 1971] and with optical emissions at 428 nm [Helliwell et al., 1980a]. Another technique, discussed in this paper, involves the observation of precipitation-induced amplitude perturbations in subionospherically propagating fixed-frequency VLF signals. This effect, first noted by Antarctic field operator M. Trimpi in 1963 and called for that reason the 'Trimpi effect,' was reported by Helliwell et al.[1973]. Similar observations of perturbations in the phase of subionospheric VLF signals have been reported by Lohrey and Kaiser [1979].

Figure 1 presents a diagram of the original Trimpi effect experiment and its interpretation. A lightning discharge in the northern hemisphere excites a whistler traveling along a magnetospheric path to a VLF receiver (R) in the Antarctic. In the wave-particle interaction region, the whistler interacts with counterstreaming energetic electrons, some of which are then precipitated into the conjugate ionospheres, either directly or after mirroring. Patches of enhanced ionization are thus created; during nighttime, their extensions below about 80-km altitude cause the reflection height for subionospheric VLF propagation to be lowered, resulting in amplitude perturbations in signals from fixed-frequency transmitters such as that marked T in the diagram. The amplitude perturbations can be positive or negative. The recovery time of a perturbation is of the order of 30 s, probably as a result of loss of electrons by attachment to neutral molecules [Dingle, 1977].

New information on electron burst precipitation has now been acquired from a data set recorded at Siple, Antarctica, and at its magnetic conjugate Roberval, Quebec, on September 11, 1973. These stations detected a series of approximately 20 VLF noise bursts and correlated amplitude perturbations of 17.8-kHz signals from the U.S. Navy VLF transmitter NAA (Cutler, Maine). Perturbations of 24.0-kHz signals from the NBA transmitter at Balboa, Canal Zone, were also observed at Siple. The correlations were similar in several respects to ones reported previously [Helliwell et al., 1973] but also exhibited important differences. While the previous events involved precipitation caused directly by whistlers, the new events were driven by relatively long (~10 s) bursts of 'noise.' Many of the noise bursts were themselves triggered by whistlers, however. Previous events developed along field lines within the plasmasphere, but the new ones involved propagation paths in the low-density plasmatrough just beyond the plasmapause. The amplitude perturbation signatures in both instances

Paper number 1A0399.
0148-0227/81/001A-0399$01.00

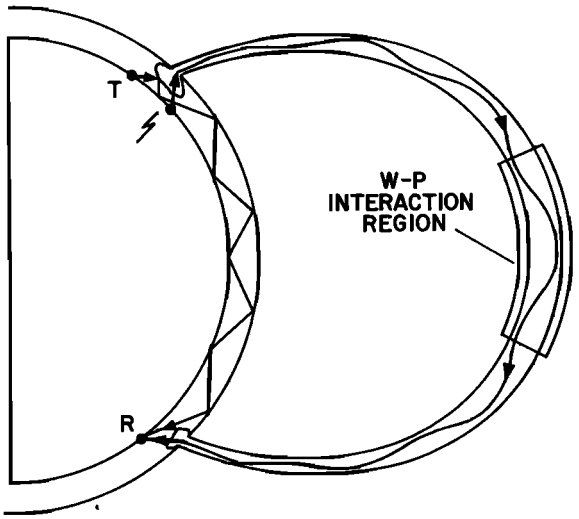

Fig. 1. Diagram of the original Trimpi effect reported by Helliwell et al. [1973]. A whistler propagating along a field-aligned path in the magnetosphere precipitates electrons into the conjugate hemispheres, thus perturbing the earth-ionosphere waveguide and the properties of signals propagating from a transmitter T to a receiver R.

had decay rates with a characteristic ~30-s time constant, but the new events had longer rise times (5-15 s) and occasionally had a long-lasting undershoot (2-5 min) during their recovery. As in the previous work, perturbations were observed on long subionospheric paths (9 and 13 Mm), but the new cases also involved a short path (600 km). The previous events were recorded in one hemisphere only, while in the present study, conjugate observations were obtained. Several of the new events are described in detail in the following section.

Experimental Results

Global features. Simultaneous broadband VLF recordings (on magnetic tape in analog form) were made at Siple and Roberval during the periods 0800-0830 and 0900-0930 UT on September 11, 1973. The main observations reported here concern these periods, and the records displayed were made by processing the taped data. Broadband recording continued at Roberval over the wider period 0800-1100 UT. A multichannel chart recorder at Siple displayed general VLF activity (including noise burst amplitudes and NAA and NBA signal strengths) on a continuous basis (but with interruptions when the Siple VLF transmitter was in operation).

The overall period of observation, ~0600-1200 UT (~0100-0700 MLT), was one of anomalously deep quieting during an otherwise moderately disturbed period. From 0600-1200 UT on September 11, K_p was 1+ and 1, following values of 4+ and 3+ in the 0000-0600 period. The sum K_p value for the preceding day was 29-.

A new feature of the data is the availability of information on the field lines of propagation of the VLF waves. These field lines were just beyond the plasmapause, at a geocentric equatorial distance of 3.65 ± 0.15 R_E. The path information was obtained from the dispersion properties of whistlers containing components propagating on both sides of the boundary and was confirmed by VLF recordings on the Explorer 45 satellite (courtesy of R. Anderson). The satellite was within a few degrees of the Siple-Roberval magnetic meridian on an outbound pass that carried it through the plasmapause about 14° north of the magnetic equator. The boundary crossing was determined from the cessation of plasmaspheric whistler propagation and the onset of narrowband noise and noise burst phenomena. (Similar OGO 1 and OGO 3 crossing determinations were described by Carpenter et al. [1969].) A number of the noise bursts observed at Siple and Roberval were also observed on the satellite. These observations will be described elsewhere.

Figure 2 shows a number of great circle paths from northern hemisphere transmitters to Siple (SI) and Roberval (RO). Those signal paths that were observably affected during the September 11 period of observation are indicated by solid curves. The intersections of these paths with the projection of the plasmapause on the ionosphere serves to locate the precipitation regions. As expected for a self-consistent picture, crossings occur between transmitters and receivers and are approximately conjugate magnetically. The longitudinal

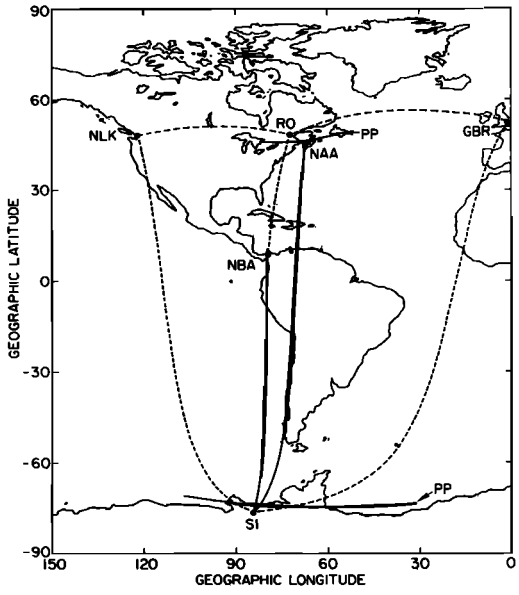

Fig. 2. Great circle paths from VLF transmitters NAA, NBA, NLK, and GBR to Roberval (RO) and to Siple (SI). Paths on which perturbations were observed on September 11, 1973, are shown by solid curves. The projection of the plasmapause onto to the ionosphere near RO and SI is shown by the curves labeled PP. These curves were determined using the geomagnetic model given by Seely [1977] who worked with a hybrid geomagnetic model that combined an international geomagnetic reference field with the Olson-Pfitzer symmetric model.

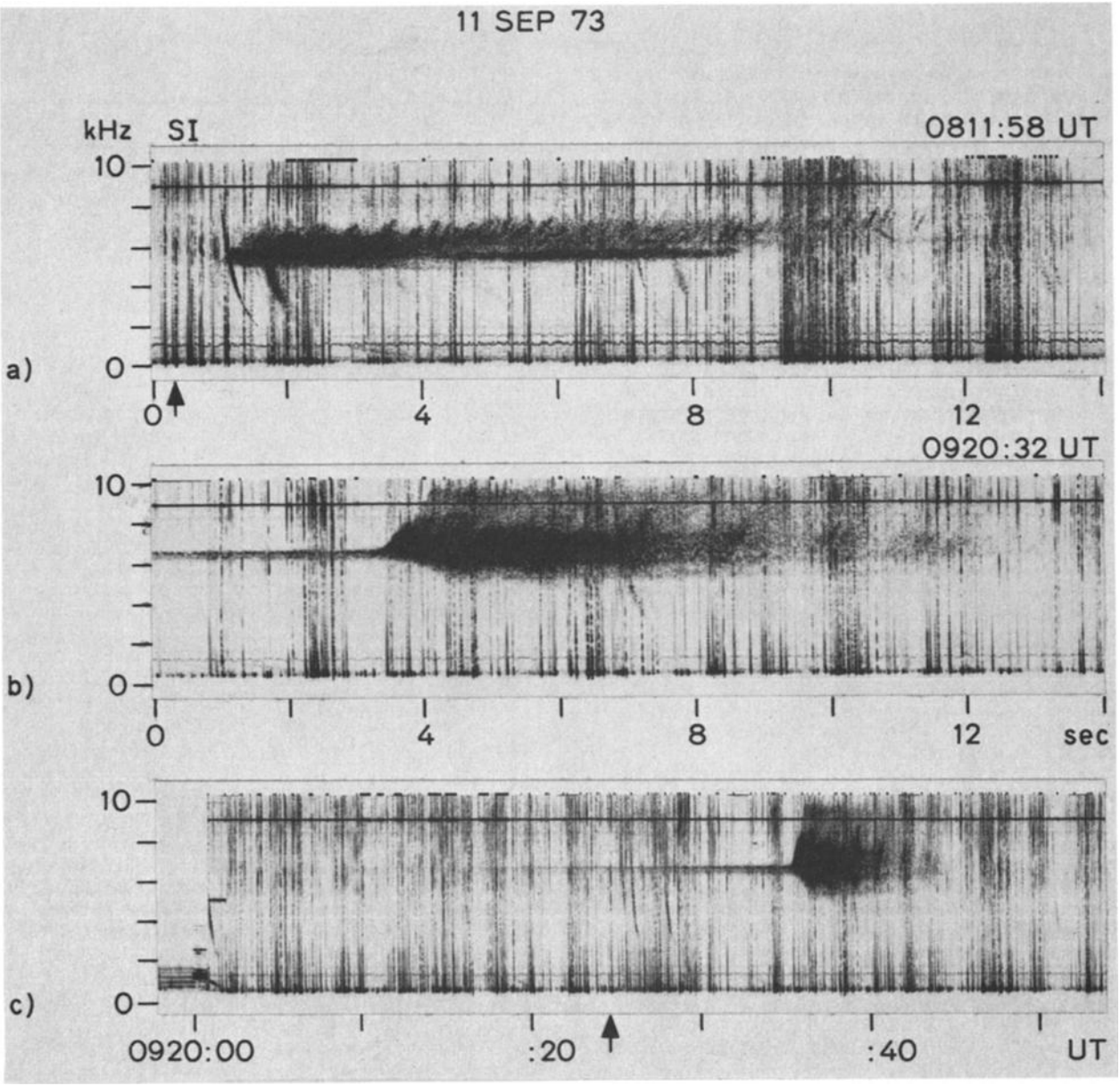

Fig. 3. Spectrographic examples of VLF noise bursts found to be correlated with amplitude perturbations of subionospheric signals. (a) Noise burst triggered directly by a whistler. (b) Noise burst showing a main body preceded by a narrowband precursor. (c) Same as Figure 3b but on a different time scale. See text for further details.

extent of the precipitation regions can be roughly estimated as less than ~10°, based on the apparent lack of effect on the NBA-RO, NLK-SI, and GBR-SI paths.

Approximately 20 noise bursts and amplitude perturbations were detected in the 0800-0930 UT period. At least 90% of these were correlated on a one-to-one basis.

Noise bursts. The noise bursts were found to occur at intervals of roughly 5 min over a several-hour period. Examples of individual bursts are shown in Figure 3. Two basic wave structures were observed: a main body of each burst and, in some cases, a precursor noise band.

The main bodies of the bursts usually developed very rapidly (within less than 1 s) and then gradually weakened with time. Typically, a burst body lasted for about 10 s, spanned a frequency range of a few kilohertz centered near 6 kHz, and consisted of closely spaced rising elements. However, the overall shape and detailed structure of the bursts varied from case to case and included prolonged elements that rose and fell, unstructured noise, and banded noise forms.

In the early part of the observation period, the main body was in most cases found to be directly triggered by a whistler component propagating just outside the plasmapause. An example of such triggering is illustrated in Figure 3a. The two clearly visible whistler traces propagated inside the plasmasphere. The triggering whistler component preceded those

traces because of its generally higher group velocity. It is only defined on the spectrogram within a narrow range near 6 kHz at ~0.6 s after the time of origin (marked by an arrow) of the whistlers. (This interpretation is based upon detailed comparisons of successive events and upon extensive research on similar phenomena.) See Carpenter [1978] for additional details of this event and for other examples of whistler triggering.

In the later part of the observation period, narrow noise bands often preceded the initiation of the main bursts. These precursors were symmetrical in form about a constant center frequency (or frequencies) and could be present for relatively long periods (~30 s). Their monochromatic structure suggests that they were magnetospheric lines of the type reported by Helliwell et al., [1973], which may possibly originate in power line harmonic radiation. The example in Figures 3b and 3c shows precursor activity centered at two frequencies separated by roughly 240 Hz. The precursors built up gradually out of the background noise level and became progressively stronger. In some cases, as in Figures 3b and c, narrowband segments of an echoing whistler were superimposed on the precursor, and these too progressively grew in amplitude. When whistler echoes were present, initiation of the main burst body coincided with the arrival of an echo. More detail on this activity is also given by Carpenter [1978].

During the periods of conjugate recording, noise bursts were usually observed at both receiving stations during each event. Early on, when direct whistler triggering was prevalent, the conjugate bursts had very different spectra with disparate magnitudes, durations, and general spectral appearances. Onset times of these early conjugate bursts occurred within a range of a second or so of each other. Later, when precursors appeared, the conjugate spectra became more similar, and for three successive bursts, triggering of the main body at Roberval occurred one whistler mode hop time (~0.6 s) after triggering at Siple. One of these latter events is illustrated in Figure 11 of Carpenter [1978].

Amplitude perturbations. The temporal signatures of the three types of subionospheric amplitude perturbation that have been observed so far are sketched in Figure 4. The whistler-induced Trimpi effect is illustrated in Figure 4a, while events of the type discussed in this report are represented by Figures 4b and 4c. All three types show an abrupt, roughly linear initial change followed by a relatively slow decay with a characteristic 30-s time constant. The rise time for the first type is typically ~2 s, corresponding to the approximate duration of a whistler. Rise times for the second and third types are longer, since the precipitation that causes them is driven by noise bursts that last for roughly 10 s. The third type is distinguished by the presence of an undershoot, such that the amplitude decays from the initial perturbation peak to a new quasi-equilibrium level below the original unperturbed amplitude. There is then a several-minute period of recovery back to the pre-event level. Note that

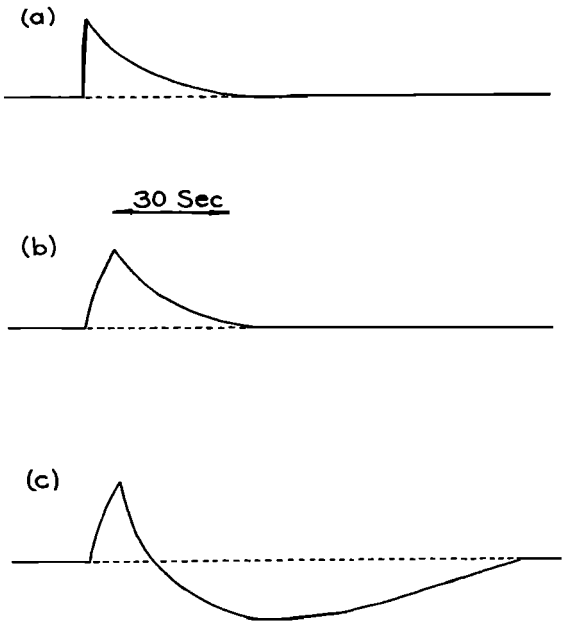

Fig. 4. Diagram of three types of amplitude perturbation signature. (a) Signature of a whistler-induced Trimpi event. (b) Long-rise-time event associated with VLF noise bursts. (c) Long-rise-time event with an undershoot during the recovery phase. In all three cases, if the perturbation is initially negative, the signature is inverted but otherwise has the same form.

if the perturbations are initially negative, the signatures as shown in Figure 4 are inverted but have the same forms. For convenience, the term 'undershoot' will be applied in both cases.

Figure 5a shows examples of amplitude perturbations of the NAA signals received at Siple. Below is the wave field strength observed at Siple in the 4.5 to 8.0-kHz band. The times of occurrence of four noise bursts are indicated by arrows at the bottom of the record. At each time there was a ~10% increase in NAA amplitude. The size of this increase did not vary markedly from event to event, but the recovery patterns of the perturbations did show variation. In the first and fourth events the perturbation signatures were like that of Figure 4b. However, the second and third events, which were associated with stronger noise bursts, exhibited the undershoot effect of Figure 4c.

Figure 6a shows amplitude perturbations of the NBA signals received at Siple. Figure 6b shows the simultaneous record of NAA at Roberval. The noise background on the Roberval broadband record (Figure 6c) is relatively high, but noise bursts can be clearly seen at the two times marked along the lower edge of the record. Noise bursts and small NAA amplitude perturbations were also detected at Siple. The NBA-SI and NAA-RO signatures are very similar in form; both exhibit the undershoot phenomenon, but in contrast to the standard event of Figure 4c and the NAA-SI signatures of Figure 5, the perturbations are inverted so that the signal

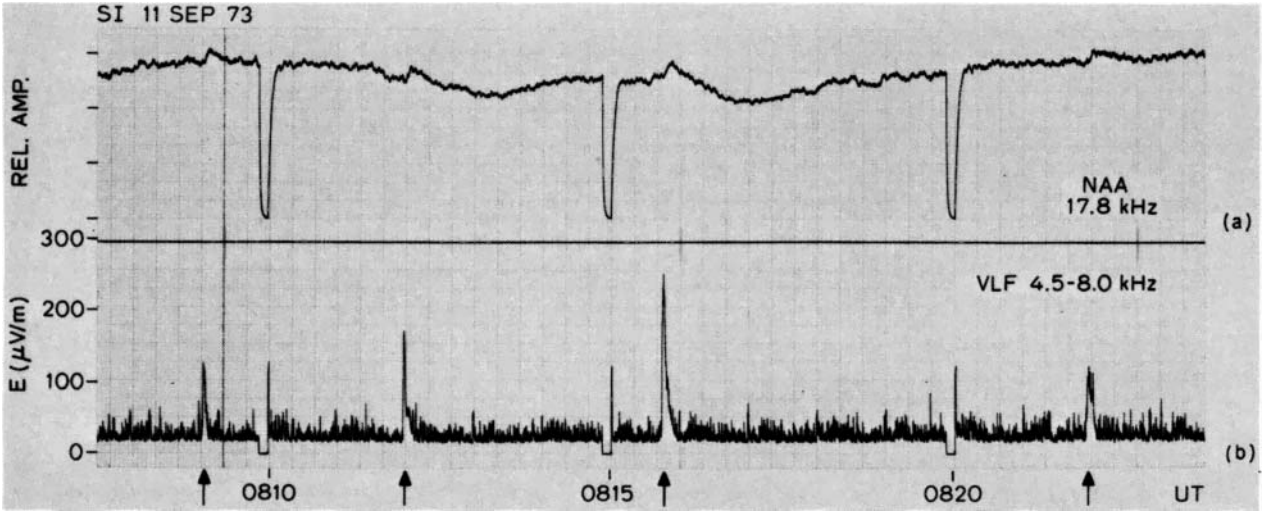

Fig. 5. Correlated examples of (a) NAA amplitude perturbations and (b) VLF noise bursts observed at Siple Station. Arrows along the lower margin of the record indicate the onset times of the events. Gaps appear in the data at 5-min intervals for timing purposes. The charge and discharge time constants of the integrator used for processing the data were 3 s and 1 s in Figure 5a and 300 ms and 100 ms in Figure 5b.

amplitude changes in the negative direction initially and in the positive direction during recovery. Near 0922 UT the undershoot magnitude was about twice that of the initial perturbation.

Figure 7 provides an expanded view of the field strength of the NBA signals propagating from the Canal Zone to Siple at the time of a double VLF burst. Figure 7a shows the NBA amplitude, Figure 7b the broadband wave amplitude from 4.5 to 8.0 kHz, and Figure 7c the corresponding broadband spectrum. A weak

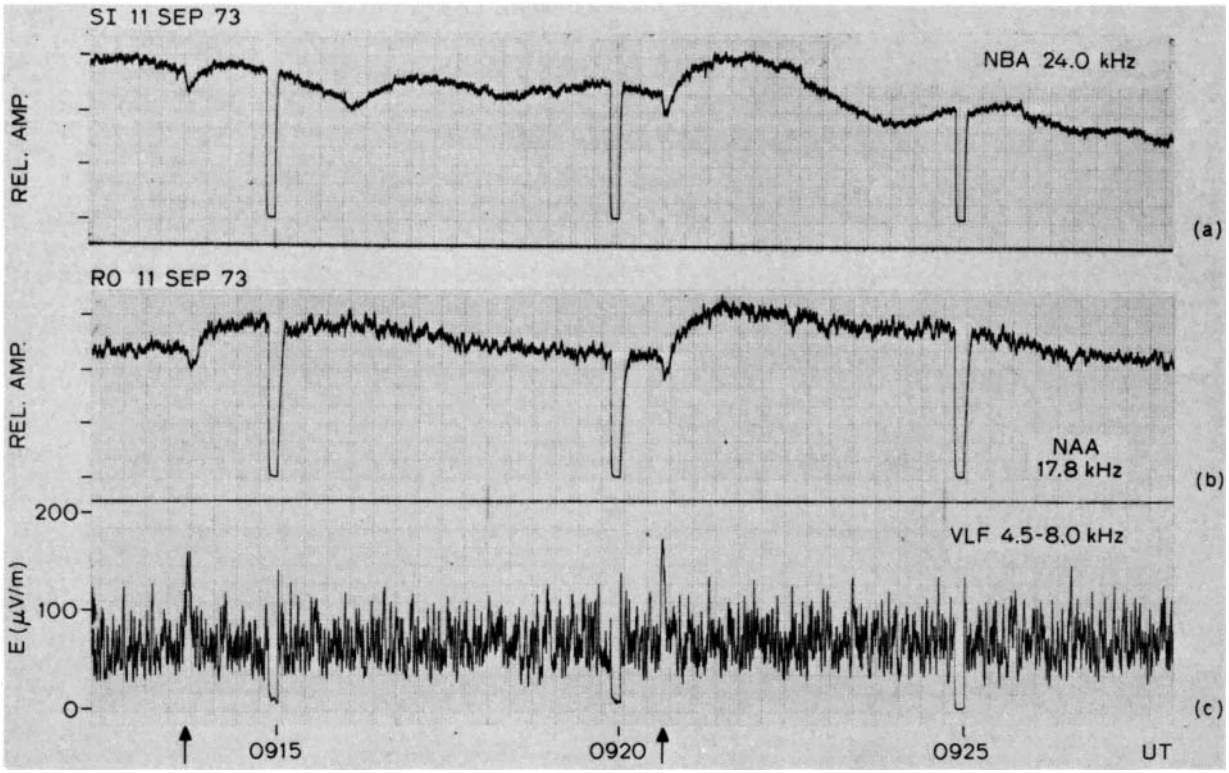

Fig. 6. Examples of amplitude perturbations observed simultaneously at conjugate stations Roberval and Siple. (a) NBA at Siple. (b) NAA at Roberval. (c) Broadband VLF field strength at Roberval. Arrows below Figure 6c indicate the onset times of VLF noise bursts. The charge and discharge time constants of the integrator used for processing the data were 1 s and 300 ms in Figure 6a, 10 s and 300 ms in Figure 6b, and 3 s and 100 ms in Figure 6c.

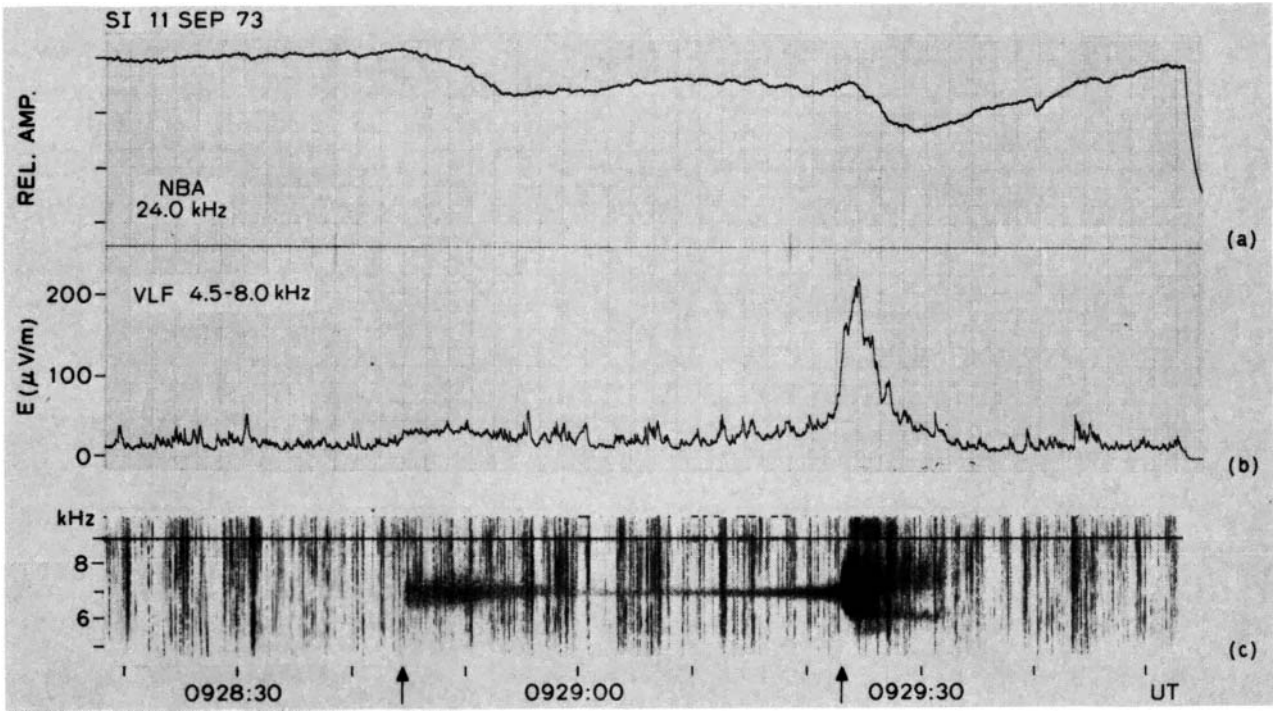

Fig. 7. A double noise burst and associated amplitude perturbations at Siple. (a) Amplitude perturbations on NBA. (b) Broadband field strength in the range 4.5-8 kHz. (c) Dynamic spectrum of 4.6-9.6 kHz. Arrows mark the onset of each part of the double noise burst. The line at 9 kHz in Figure 7c is a timing signal. The charge and discharge time constants of the integrator used for processing the data were 3 s and 1 s in Figure 7a, and 300 ms and 100 ms in Figure 7b.

noise burst began at the time of the first arrow below Figure 7c and after ~10 s decayed into a precursor-type noise band. During this initial burst, there was a near-linear decrease in the NBA signal level. At the time of the second arrow, the main body of the second burst developed rapidly, reaching a peak amplitude roughly 13 times that of the first part of the event. During the second burst there was another near-linear decrease in the NBA signal level. The slope of the decrease was larger than that observed during the first event by a factor of ~3. Between bursts, only limited recovery of the NBA level took place. Following the second burst, an apparently normal recovery began (perhaps with undershoot, but an interruption in the recording prevented observation of its completion).

Amplitude perturbations were usually observed in both hemispheres for each precipitation event. The perturbation signatures were generally similar in shape, but their size and sense (positive or negative) varied, as did the presence or absence of undershoot. After local sunrise in the northern ionosphere at ~0930 UT, perturbations were no longer seen at Roberval, although the noise bursts continued to occur. Perturbations were seen at Siple until local sunrise at ~1030 UT.

Discussion

Global features. Regarding noise burst precipitation between conjugate points, the restricted bandwidths of the precursors and the occurrence of whistler echoing suggest propagation in a limited region such as a duct. However, a report on propagation just outside the plasmapause [Carpenter, 1978] revealed whistler activity, including echoing, at frequencies above the half-equatorial-gyrofrequency limit normally associated with ducts [Carpenter, 1968]. So the noise burst propagation may not be ducted in the usual sense. Guided propagation along the density gradient that forms the plasmapause should be possible, and Inan and Bell [1977] have indeed found that nonducted propagation between conjugate ionospheres could occur just beyond the plasmapause for wave normals near the Gendrin angle. Excitation of the required large wave normal angles from the ground has also been found possible (U. S. Inan, private communication, 1980).

Precipitated electrons must have energies greater than about 100 keV in order to penetrate to the lower D region ($\lesssim$80 km), where the rapid attachment of electrons to neutrals thought to be required for the observed recovery times can occur [Dingle, 1977]. Cyclotron resonance calculations covering the range of the measured parameters show that the noise bursts could have resonated in the near-equatorial magnetosphere with 100-keV electrons at the edge of the loss cone. For example, using a background electron density of 30 cm^{-3} at 3.65 R_E equatorial distance (as estimated from whistler measurements) and a representative noise burst frequency of 6.5 kHz, it was found that the min-

imum resonant electron energy (i.e., the energy that gives resonance exactly at the equator) was 23 keV and that the resonance point for 100-keV electrons was located 17° from the equator.

It has been assumed that sufficient precipitated flux was produced by each noise burst to lower the effective VLF reflection height in the earth-ionosphere waveguide to ~75 km. This requires generation of ~500 el cm^{-3} at that altitude (see discussion by Potemra et al. [1967]). Indications that this requirement was met in the present case come from a study by Foster and Rosenberg [1976] of precipitation events observed near Siple Station on January 2, 1971. In those events, X ray bursts were correlated on a one-to-one basis with 2 to 4-kHz VLF chorus bursts that were found to propagate a few tenths of an L value beyond the plasmapause [Rosenberg et al., 1971]. On the basis of the X ray measurements, Foster and Rosenberg estimated that a typical downward precipitated flux parallel to the geomagnetic field was $10^4 \exp [-(E - 40)/45]$ cm^{-2} s^{-1} keV^{-1} for E in keV. This represents about 0.03 erg cm^{-2} of precipitated energy greater than 100 keV. Assuming this energy was deposited between 70 and 80 km and that one ion pair was produced for each 35 eV, an estimated production rate of ~500 el/cm^{-3} s^{-1} near 75 km results. A similar level of production might be expected for the September 11, 1973, events. Absolute wave amplitude data from January 2, 1971, are not available, but Helliwell et al. [1980a], reporting wave-optical burst correlations at Siple in 1977, found wave amplitudes comparable to the ~150 μV/m reported here. The electron production rate might have been lower on September 11, 1973, than on January 2, 1971, due to quieter conditions and a consequently reduced trapped flux intensity, but the September 11 noise bursts lasted considerably longer, leading us to expect that the excess electron density at ~75 km was sufficient to lower the VLF reflection height to that altitude.

The events occurred at roughly 5-min intervals over the several-hour observing period. Since the whistlers which triggered many of the noise bursts occurred at a much faster rate (several per minute) and since the period was one of deep magnetic quieting, it is assumed that the time separation of the events was governed primarily by magnetospheric particle dynamics.

For the first time, amplitude perturbations were seen simultaneously in both hemispheres, showing that comparable precipitation effects can occur in both the conjugate ionospheres in spite of the differences in particle mirror heights over Roberval and Siple and the resulting difference in equatorial loss cone width. An ideal dipole field line with geocentric equatorial distance of 3.65 R_E is symmetrical and has an equatorial loss cone of about 6.3° in half width. The actual asymmetrical field line produces asymmetrical northern and southern loss cones, the northern loss cone being narrower by about 0.4° at the equator (based on data given by Seely [1977]). The occurrence of significant precipitation in the northern hemisphere implies that wave amplitudes were strong enough to lower electron pitch angles more than 0.4° and to scatter some particles into the narrower loss cone. Using the scattering analysis by Dingle [1977], an equatorial density of 30 cm^{-3}, and a wave frequency of 6.5 kHz, the wave amplitude required to precipitate electrons with energies of 100 keV and higher was found to be at least 30 pT. Amplitudes of this magnitude have previously been measured for natural emissions observed by satellite [Burtis and Helliwell, 1975] and are also expected to result from temporal growth of coherent signals injected into the magnetosphere from man-made sources [Helliwell, 1979].

Also for the first time, amplitude perturbations were seen on a short subionospheric path (NAA to RO, about 600 km). This shows that perturbations can occur without the subionospheric VLF path being restricted to one or two waveguide modes, as was probably the case for the long paths of the present and previous observations. And because perturbation signatures were similar on both short and long paths, the shape of the signatures would appear to be governed primarily be ionospheric changes and not by the mechanism of subionospheric propagation. Note, however, that the sense (positive or negative) and the magnitude of the signal perturbations do depend upon the propagation mechanism [Dingle, 1977; Lohrey and Kaiser, 1979]; that is, it may depend upon focusing and defocusing of a single waveguide mode [Dingle, 1977] or, if additional modes are important [Lohrey and Kaiser, 1979], upon the manner in which the modes are differentially affected by the precipitation.

Perturbations disappeared on the NAA-RO path after local sunrise, confirming earlier observations by Helliwell et al. [1973] based on whistler-driven events. The effect was made particularly clear by the fact that the driving noise bursts continued to occur after sunrise and, moreover, continued to produce amplitude perturbations on paths that remained west of the terminator. Probably, the higher electron concentration in the sunlit regions of the ionosphere lowered the VLF reflection height below altitudes significantly affected by the burst precipitation.

It is not yet known how frequently the type of precipitation activity described here occurs. The present case study is the only one of its kind thus far; it was made possible by a combination of observing conditions that are difficult to reproduce (e.g., plasmapause projection several hundred kilometers equatorward of Roberval, sudden quieting, nighttime ionosphere in both hemispheres, etc.). However, it is believed that burst precipitation does occur just beyond the plasmapause on at least several days each month, probably at various intervals ranging from seconds to tens of minutes. Noise forms similar to those reproduced here, but with various temporal separations, have been observed on several days each month at an L ~ 4 ground station [Carpenter, 1978].

Noise bursts. Signals transmitted from Siple Station to the northern hemisphere along magnetospheric paths within the plasmasphere have demonstrated a threshold in transmitted power for occurrence of rapid temporal growth and for triggering of emissions, and this threshold level varies with time [Helliwell et

al., 1980b]. Echoes of the transmitted signals traveling the same magnetospheric paths have been shown to reduce the received signal levels [Raghuram et al., 1977]. For purposes of interpreting the present noise burst observations, the magnetosphere is therefore considered to act as a narrowband VLF amplifier that can become unstable above a threshold input level [e.g., Helliwell, 1979]. Amplifier gain (and hence the instability threshold) varies according to the supply of energetic trapped electrons and the presence of any quasi-coherent wave energy that can affect the arrangement of these electrons. Temporal variations in the trapped electron distribution along the plasmapause are assumed to have provided significant amplifier gain at roughly 5-min intervals. We then hypothesize that direct whistler triggering occurred early in the observation period when the threshold for instability was less than whistler power levels. Later the threshold rose, possibly as a result of a different electron distribution or better wave echoing conditions that caused gain suppression. Whistlers were not then strong enough to initiate instability, and weak power line radiation and/or echoing whistler wave packets could be progressively amplified so that precursor bands developed. Eventually, the precursors became strong enough to initiate instability. The main bursts were eventually quenched either by the ~5-min changes in the electron supply or perhaps by internal electron disorganization brought about by the amplification/oscillation process.

In contrast to the noise burst observations, Siple triggering of emissions within the plasmasphere usually produces only one or a few distinct narrowband emissions at a time, but this process can often be repeated with intervals of less than a second between events [Helliwell and Katsufrakis, 1974, 1978].

Because of the apparent importance of weak injected signals in the precursor process, Siple transmitter signals might be expected occasionally either to initiate or otherwise to catalyze a similar process. On April 6, 1977, this appears to have occurred; a fifth harmonic of a Siple signal initiated a constant-frequency precursor that developed into a noise burst. The radiated power was comparable to the few watts used in successful simulations of radiation from power lines [Park and Chang, 1978]. More details of this event will be reported elsewhere. It has also been noted that precursor development resembles the buildup of various echoing wave forms within the plasmasphere, such as periodic emissions [Helliwell, 1965] and magnetospheric line radiation events (C. G. Park, private communication, 1980).

Amplitude perturbations. A new feature of the present data is the long rise time (~10 s) of the amplitude perturbations corresponding to the relatively long duration of the noise bursts. During this time the trapped electrons along the active field lines underwent several bounces, and hence the individual electrons encountered the wave more than once. Since the perturbations continued to grow during this period at a roughly constant rate, precipitation must have been continuous and roughly constant in rate, and trapped fluxes near the loss cone must have been maintained. This suggests that future experiments using strong VLF signals from a space-borne transmitter may be able to induce controlled precipitation of electrons for significant periods of time. Theoretical calculations of the precipitation produced by long pulses [Dingle, 1977; Helliwell, 1979] support this suggestion.

The near-linear onset and consistent shape of the perturbation signatures suggest that a good first-order model for a precipitated flux burst is an energy-integrated time-rectangular pulse and that the slope of the corresponding perturbation onset is proportional to the intensity of that pulse. Treating the noise bursts as rectangular pulses at a constant frequency and noting that the total precipitation they produce is then a linear function of the noise amplitude [Dingle, 1977], the perturbation onset slopes should also be linearly related to noise amplitude (provided that the trapped flux and subionospheric propagation conditions do not change). However, this proportionality will not necessarily hold if a single noise burst precipitates flux into both hemispheres or if conjugate noise bursts both contribute flux to the same hemisphere. Cases demonstrating a lack of proportionality are discussed below.

Although the relation between noise burst amplitudes and the size of corresponding subionospheric perturbations has not yet been investigated in detail, there is limited evidence of a saturation effect. The slope (and size) of the initial perturbation of each of the four events of Figure 5 is about the same, although the noise burst amplitudes vary over a range of more than 2:1. Existence of a double loss cone makes saturation possible for precipitation in the southern hemisphere of electrons that have first mirrored in the northern hemisphere. These electrons travel in the gap between the northern and southern loss cones, and for large enough wave amplitudes, an increase in wave amplitude in effect just shifts more electrons through the gap into the narrower northern loss cone, leaving the number in the gap unchanged. In order that the saturation effect not be masked, direct precipitation in the south caused by northward traveling wave bursts must be relatively weak. The northgoing bursts received at Roberval were indeed weak for the last three events of Figure 5, but a relatively large burst appeared during the first event. Additional measurements and/or more examples are required to firmly establish the presence of this type of saturation.

In the Siple data of Figure 7 the two parts of the double noise burst have an amplitude ratio of ~13:1, while the slopes of the corresponding amplitude perturbations on NBA indicate a precipitation ratio of only ~3:1. To account for this discrepancy, some of the flux precipitated by the second part of the burst must have been deposited in the northern hemisphere, and/or there must have been a north going double noise burst that contributed a higher proportion of flux to the first amplitude perturbation. Examination of the Roberval records shows both a double noise burst with amplitude ratio ~2:1 and northern precipitation during the second

part of the burst. Hence the NBA perturbations at Siple are probably the combined result of direct and mirrored precipitation bursts.

Undershoot was possibly the result of background drizzle precipitation from a duct being cut off by the noise bursts. The bursts could have depleted trapped electrons near the loss cone or destroyed wave amplification properties along the duct. Recovery from this situation would have occurred as the perturbed trapped flux distribution drifted longitudinally out of the duct. The drift rate for 100-keV electrons is about 100 km/min when referred to ionospheric altitudes, so that the observed recovery times of 2-5 min imply east-west duct widths of 200-500 km. This order of magnitude is consistent with duct width estimates made be Angerami [1970] and with the ~10° maximum longitudinal extent estimated for the subionospheric disturbances. (Recall, however, that propagation just beyond the plasmapause may not be ducted in the usual sense.) The ~5-min separation of the noise bursts may also be related to drift of the perturbed trapped flux distribution out of a duct. Raghuram et al., [1977] discuss a similar mechanism of amplification reduction and drift recovery as an explanation for the 'quiet band' phenomenon, whereby Siple signals suppressed preexisting noise activity in a narrow band below the transmitted frequency.

Another possible explanation for undershoot involves a buildup of positive ions in the ionosphere following successive noise bursts. This might lead to a lowered equilibrium electron concentration through increased recombination loss. Investigation of the undershoot phenomenon is continuing.

Acknowledgments. The events reported here were discovered by J. Yarbrough while analyzing the broadband VLF data for another study. The authors are indebted to him for his interest and resourcefulness. We thank R. A. Helliwell, U. S. Inan, and T. F. Bell for valuable discussions and comments. We are grateful to J. P. Katsufrakis for his supervision of the Stanford field program, to E. Paschal and W. Trabucco for their excellent operational work at Siple Station, and to G. Daniels and K. Dean for assistance in preparation of the typescript. This work was sponsored in part by the Office of Naval Research under grant N00014-76-0689, in part by the Division of Polar Programs of the National Science Foundation under grants DPP76-82646 and DPP78-05746, and in part by the Atmospheric Sciences Division of the National Science Foundation.

The Editor thanks S. Kaye and S. D. Shawhan for their assistance.

References

Angerami, J. J., Whistler duct properties deduced from VLF observations made with the OGO 3 satellite near the magnetic equator, J. Geophys. Res., 75, 6115, 1970.

Burtis, W. J., and R. A. Helliwell, Magnetospheric chorus: Amplitude and growth rate, J. Geophys. Res., 80, 3265, 1975.

Carpenter, D. L., Ducted whistler mode propagation in the magnetosphere: A half-gyrofrequency upper intensity cutoff and some associated wave growth phenomena, J. Geophys. Res., 73, 2919, 1968.

Carpenter, D. L., Whistlers and VLF noises propagating just outside the plasmapause, J. Geophys. Res., 83, 45, 1978.

Carpenter, D. L., C. G. Park, H. A. Taylor, Jr., and H. C. Brinton, Multiexperiment detection of the plasmapause from OGO satellites and Antarctic ground stations, J. Geophys. Res., 74, 1837, 1969.

Dingle, B., Burst precipitation of energetic electrons from the magnetosphere, Ph.D. Thesis, Stanford University, Stanford, Calif., 1977.

Foster, J. C., and T. J. Rosenberg, Electron precipitation and VLF emissions associated with cyclotron resonance interactions near the plasmapause, J. Geophys. Res., 81, 2183, 1976.

Helliwell, R. A., Whistlers and Related Ionospneric Phenomena, Stanford University Press, Stanford, Calif., 1965.

Helliwell, R. A., Siple Station experiments on wave-particle interactions in the magnetosphere, in Wave Instabilities in Space Plasmas, edited by P. J. Palmadesso and K. Papadopoulos, p. 191, D. Reidel, Hingham, Mass., 1979.

Helliwell, R. A., J. P. Katsufrakis and M. L. Trimpi, Whistler-induced amplitude perturbation in VLF propagation, J. Geophys. Res., 78, 2679, 1973.

Helliwell, R. A., and J. P. Katsufrakis, VLF wave injection into the magnetosphere from Siple Station, Antarctica, J. Geophys. Res., 79, 2511, 1974.

Helliwell, R. A , and J. P. Katsufrakis, Controlled wave-particle interaction experiments, in Upper Atmosphere Research in Antarctica, Antarctic Res. Ser., vol. 29, edited by L. J. Lanzerotti and C. G. Park, AGU, Washington, D. C., 1978.

Helliwell, R. A., S. B. Mende, J. H. Doolittle, W. C. Armstrong, and D. L. Carpenter, Correlations between λ4278 optical emissions and VLF wave events observed at L ~ 4 in the Antarctic, J. Geophys. Res., 85, 1194, 1980a.

Helliwell, R. A., D. L. Carpenter, and T. R. Miller, Power threshold for growth of coherent VLF signals in the magnetosphere, J. Geophys. Res., 85, 3360, 1980b.

Inan, U. S., and T. F. Bell, The plasmapause as a VLF waveguide, J. Geophys. Res., 82, 2819, 1977.

Lohrey, B., and A. B. Kaiser, Whistler-induced anomalies in VLF propagation, J. Geophys. Res., 84, 5121, 1979.

Park, C. G., and D. C. D. Chang, Transmitter simulation of power line radiation effects in the magnetosphere, Geophys. Res. Letts., 5, 861, 1978.

Potemra, T. A., A. J. Zmuda, C. R. Haave, and B. W. Shaw, VLF phase perturbations produced by solar protons in the event of February 5, 1965, J. Geophys. Res., 72, 23, 1967.

Raghuram, R., T. F. Bell, R. A. Helliwell, and J. P. Katsufrakis, Quiet band produced by VLF transmitter signals in the magnetosphere, Geophys. Res. Letts., 4, 199, 1977.

Rosenberg, T. J., R. A. Helliwell, and J. P. Katsufrakis, Electron precipitation associated with discrete very low frequency emissions, J. Geophys. Res., 76, 8445, 1971.
Seely, N. T., Whistler propagation in a distorted quiet-time model magnetosphere, Tech. Rep. 3472-1, Stanford Electr. Lab., Stanford Univ., Stanford, Calif., 1977.

(Received May 22, 1980;
revised March 3, 1981;
accepted March 5, 1981.)